Available online at www.sciencedirect.com
ScienceDirect
International Journal of Heat and Mass Transfer 50 (2007) 3007–3018
International Journal of HEAT and MASS TRANSFER
www.elsevier.com/locate/ijhmt

Dimensional analysis of thermo-fluid-dynamics of high hydrostatic pressure processes with phase transition

W. Kowalczyk *, A. Delgado

Lehrstuhl für Strömungsmechanik, Universität Erlangen-Nürnberg, Cauerstr. 4, D-91058 Erlangen, Germany

Received 6 October 2005; received in revised form 30 November 2006
Available online 26 February 2007

Abstract

In the current paper the dimensional analysis of thermo-fluid-dynamic mechanisms taking place during high pressure treatment of bio-substances is carried out. Both forced and free convection case is described. Additionally, the phase change in the pressurized medium is considered. The significance of several terms in the conservation equation of momentum and energy is estimated. Especially in systems with low velocity of fluid some terms in the governing equations can be neglected, e.g. irreversible transformation of kinetic in thermal energy. The dimensionless numbers/groups that describe the fluid flow and phase transition at high hydrostatic pressure are determined.

Keywords: High hydrostatic pressure; Dimensional analysis; Phase change; Free convection; Forced convection

1. Introduction

The high pressure technology opens many possibilities for the developing of new processes and products in the food and pharmaceutical industry sector. The high hydrostatic pressure enables more careful treatment of raw materials in comparison to traditional "temperature–time" processes. The application of pressure up to 1 GPa can be used for inactivation of enzymes, alteration of texture and structure, sterilization and pasteurization and supporting of phase transitions in bio-substances. Fig. 1 shows schematically the principle of high pressure batch processing.

At the beginning of high pressure treatment the bio-substance is placed in a high pressure chamber and compressed up to a certain pressure level. Subsequently the constant pressure is held during a specified time. The pressure level and the pressure holding time differs for diverse applications. After pressurizing the decompression to ambient pressure occurs. Bio-substance can be processed either in a packed or in unpacked form. Obviously, liquid substances can serve as a pressure transferring medium themselves.

There are many literature positions describing investigations of the high pressure technology. Starting with works of Bridgman [1,2] and coming to publications of the last 15 years the general principles of high pressure processing of different substances and the effect of high pressure on their individual components [3,4] are described. Additionally, advantages and important possibilities of high pressure treatment of food are reported by Knorr [5].

For investigation of the high pressure process experimental in situ methods are also used. These methods are applied by Först et al. [6,7] in order to define the viscosity of water and aqueous solutions under high pressure. Pehl et al. [8,9] apply in situ methods for visualization of temperature and velocity distributions in liquid bio-substances during high pressure treatment. The observations of temperature and velocity fields reveal that due to local temperature differences the high pressure treatment is not homogeneous in the whole volume of the pressurized medium [10].

* Corresponding author. Tel.: +49 9131 85 29571; fax: +49 9131 85 29579.
E-mail address: kowalczyk@lstm.uni-erlangen.de (W. Kowalczyk).

0017-9310/$ - see front matter © 2007 Elsevier Ltd. All rights reserved.
doi:10.1016/j.ijheatmasstransfer.2006.12.004

Nomenclature

a	thermal diffusivity
Ar	Archimedes number
c_p	specific thermal capacity with constant pressure
D	diameter
D_t	deformation velocity tensor
Da	Darcy number
e	specific energy
Ec	Eckert number
f	mass fraction
F_G	volume force
Fr	Froude number
g	gravity
Gr	Grashof number
h	specific enthalpy
H	total enthalpy
$\widehat{H}$	specific total enthalpy
$\overline{H}$	specific total enthalpy without crystallization enthalpy
$\widetilde{H}$	enthalpy of crystallization
K	porosity function
K_0	permeability
L	characteristic length
L_f	latent heat
p	pressure
Pr	Prandtl number
q	vector of the heat flow density
$\vec{R}$	force of resistance
Re	Reynolds number
S	entropy
S_k	source term (phase transition)
Ste	Stefan number
T	temperature
$\widehat{T}$	stress tensor
ΔT	temperature difference
t	time
t_c	compression time
t_p	process time
t_s	conversion time
u	specific internal energy
v	specific volume
V	volume
$\vec{W}$	velocity vector
W_x	velocity in x-direction
W_y	velocity in y-direction
W_z	velocity in z-direction
W_0	initial velocity
x, y, z	cartesian coordinates
Δ	Laplace operator
∇	Nabla operator

Greek symbols

α	thermal expansion coefficient
δ	unit tensor
β	compressibility
ν	kinematic viscosity
λ	heat conductivity
ρ	density
η	dynamic viscosity
τ	viscous stress tensor
ξ	volume fraction
ζ	second coefficient of viscosity
Φ	dissipation function
θ	dimensionless temperature ratio
Π_A	dimensionless number – buoyancy
Π_D	dimensionless number – dissipation function
Π_P	dimensionless number – permeability of mushy region
Π_T	dimensionless number – temperature increase due to compression
Π_V	dimensionless number – influence of volume forces on energy balance

Indices

dyn	dynamic
tot	total
l	liquid
*	dimensionless value
0	initial value
s	solid
stat	static
w	wall

Hartmann et al. [11,12] investigated the convective and diffusive transport effects under high pressure by means of numerical simulation. The authors observed process inhomogenities during inactivation of enzymes and microorganisms.

The most important aspects of high pressure supported phase changes can be found in Bridgman [13], Cheftel et al. [14] or Kalichevsky et al. [15]. The background of investigations of high pressure phase transitions for biosubstances with dominating water content is the phase diagram of water. Fig. 2 illustrates the phase diagram of water up to 500 MPa with some schematically drawn possibilities of phase transition under high pressure.

The mathematical description and modelling of heat and mass transfer during solidification at normal pressure is widely reported by Voller [16], Voller et al. [17,18], Swaminathan and Voller [19], Bennon and Incropera [20,21] or Ni and Incropera [22,23]. Kowalczyk et al. [24] as first applied the enthalpy porosity method for the mathematical modelling and numerical simulation of water–ice phase changes at both normal and high pressure. In the current contribution a detailed dimensionless analysis of the high

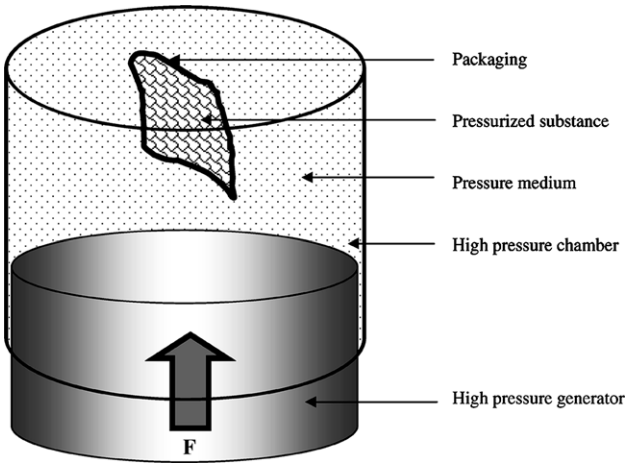

Fig. 1. Schematic illustration of high pressure treatment of bio-substances.

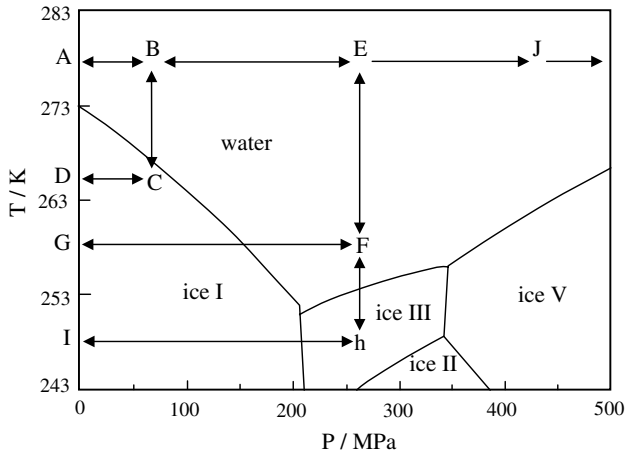

Fig. 2. Pressure temperature diagram of water with possible phase transition processes. ABCD – high pressure assisted freezing/thawing, ABEFG – high pressure induced freezing/thawing, ABEFHI – high pressure assisted freezing/thawing with the phase change between ice I and ice III, ABEJ – phase change of water in the temperatures above 273 K.

pressure processes is carried out. The dimensionless description focuses on generalization of statements about the thermo-fluid-dynamical mechanisms occurring during high pressure treatment. The processes both with forced and free convection accompanied by phase transition of pressurized medium are considered.

2. Governing equations

This paper focuses on mathematical and dimensionless description of high pressure processes and specification of effects due to compression of pressurized medium. The conservation equations of mass, energy and momentum for compressible media build the basis for the mathematical model. It is assumed that the pressurized substance is a Newtonian fluid and materially homogeneous. Moreover, the fluid is chemically inert and electrically uncharged. The mathematical definition is carried out with Cartesian coordinates. The governing equations for compressible medium are written as follow.

2.1. Conservation equation of mass

$$\frac{\partial \rho}{\partial t} + \nabla \cdot (\rho \vec{W}) = 0. \tag{1}$$

2.2. Conservation equation of momentum

$$\rho \left[\frac{\partial \vec{W}}{\partial t} + (\vec{W} \cdot \nabla) \vec{W} \right] = \nabla \cdot \widehat{T} + \vec{F} \tag{2}$$

with the specific gravitational force

$$\vec{F} = \vec{F}_{\mathrm{G}} = \rho \vec{g} \tag{3}$$

and total stress tensor

$$\widehat{T} = -p\delta + \tau. \tag{4}$$

The viscous stress tensor is defined as

$$\begin{aligned} \tau &= \left(\zeta - \frac{2}{3}\eta \right) (\nabla \cdot \vec{W}) \delta + \eta \left(\nabla \vec{W} + (\nabla \vec{W})^{\mathrm{T}} \right) \\ &= \left(\zeta - \frac{2}{3}\eta \right) (\nabla \cdot \vec{W}) \delta + 2\eta D_t \end{aligned} \tag{5}$$

with the second viscosity coefficient

$$\zeta = \eta' + \frac{2}{3}\eta \tag{6}$$

and the symmetrical deformation velocity tensor

$$D_t = \frac{1}{2} \left[\nabla \vec{W} + (\nabla \vec{W})^{\mathrm{T}} \right]. \tag{7}$$

2.3. Conservation equation of energy

The description of the energy balance for a system can be carried out differently. A possible formulation refers to the specific total energy

$$e = u + \frac{\vec{W}^2}{2}, \tag{8}$$

whereby e is the sum of the internal and kinetic energy. In this situation the conservation equation of energy in differential form can be written as

$$\rho \frac{\mathrm{D}u}{\mathrm{D}t} + \rho \frac{\mathrm{D}}{\mathrm{D}t} \left(\frac{\vec{W}^2}{2} \right) = -\nabla \cdot q + \nabla \cdot \left(\widehat{T} \vec{W} \right) + \rho \vec{g} \cdot \vec{W}. \tag{9}$$

In the first term on the right side of the energy equation q denotes the vector of heat flow (Fourier law)

$$q = -\lambda \nabla T. \tag{10}$$

In many practical applications, e.g. in codes for numerical simulation (CFD) the energy balance is used in an enthalpy

formulation. In order to convert Eq. (9) into the enthalpy equation the specific enthalpy is defined as

$$h = u + pv = u + \frac{p}{\rho}. \tag{11}$$

Insertion of Eqs. (10) and (11) into Eq. (9) and considering the decomposition of the stress tensor according to Eq. (4) results in the following enthalpy equation:

$$\rho\frac{\mathrm{D}h}{\mathrm{D}t} + \rho\frac{\mathrm{D}}{\mathrm{D}t}\left(\frac{\vec{W}^2}{2}\right) - \rho\frac{\mathrm{D}}{\mathrm{D}t}\left(\frac{p}{\rho}\right) = \nabla\cdot(\lambda\nabla T) - p\nabla\cdot\vec{W} - \vec{W}\cdot\nabla p + \nabla\cdot\left(\tau\cdot\vec{W}\right) + \rho\vec{g}\cdot\vec{W}. \tag{12}$$

Defining the specific total enthalpy

$$\widehat{H} = h + \frac{\vec{W}^2}{2} \tag{13}$$

and applying the product rule to the third term of the left side of Eq. (12) results in

$$\rho\frac{\mathrm{D}\widehat{H}}{\mathrm{D}t} - \frac{\mathrm{D}p}{\mathrm{D}t} + \frac{p}{\rho}\frac{\mathrm{D}\rho}{\mathrm{D}t} = \nabla\cdot(\lambda\nabla T) - p\nabla\cdot\vec{W} - \vec{W}\cdot\nabla p + \nabla\cdot\left(\tau\cdot\vec{W}\right) + \rho\vec{g}\cdot\vec{W}. \tag{14}$$

Some further mathematical transformations in the second and third term lead finally to

$$\frac{\partial}{\partial t}\left(\rho\widehat{H}\right) + \nabla\cdot\left(\rho\vec{W}\widehat{H}\right) = \frac{\partial p}{\partial t} + \nabla\cdot(\lambda\nabla T) + \nabla\cdot\left(\tau\cdot\vec{W}\right) + \rho\vec{g}\cdot\vec{W}. \tag{15}$$

The energy balance can be also presented in a formulation for temperature. On the basis of the enthalpy equation for the specific enthalpy

$$\rho\frac{\mathrm{D}h}{\mathrm{D}t} - \frac{\mathrm{D}p}{\mathrm{D}t} = \nabla\cdot(\lambda\nabla T) + \eta\Phi \tag{16}$$

and under consideration that

$$\frac{\mathrm{D}h}{\mathrm{D}t} = \left(\frac{\partial h}{\partial p}\right)\Big|_T\frac{\mathrm{D}p}{\mathrm{D}t} + \left(\frac{\partial h}{\partial p}\right)\Big|_\mathrm{p}\frac{\mathrm{D}T}{\mathrm{D}t} = \frac{1}{\rho}(1-\alpha T)\frac{\mathrm{D}p}{\mathrm{D}t} + c_\mathrm{p}\frac{\mathrm{D}T}{\mathrm{D}t} \tag{17}$$

the thermal energy equation is written as

$$c_\mathrm{p}\rho\frac{\mathrm{D}T}{\mathrm{D}t} = \alpha T\frac{\mathrm{D}p}{\mathrm{D}t} + \nabla\cdot(\lambda\nabla T) + \eta\Phi. \tag{18}$$

The third expression of the right side of Eq. (18) contains the dissipation function

$$\Phi = 2\left[\left(\frac{\partial W_x}{\partial x}\right)^2 + \left(\frac{\partial W_y}{\partial y}\right)^2 + \left(\frac{\partial W_z}{\partial z}\right)^2\right] + \left(\frac{\partial W_y}{\partial x} + \frac{\partial W_x}{\partial y}\right)^2 + \left(\frac{\partial W_z}{\partial y} + \frac{\partial W_y}{\partial z}\right)^2 + \left(\frac{\partial W_x}{\partial z} + \frac{\partial W_z}{\partial x}\right)^2 - \frac{2}{3}\left(\frac{\partial W_x}{\partial x} + \frac{\partial W_y}{\partial y} + \frac{\partial W_z}{\partial z}\right)^2. \tag{19}$$

3. Governing equations for the phase transition under high pressure

In the current paper the phase change problem is modelled with the enthalpy porosity method, e.g. [19,20]. The derivation of the complete model demands some assumptions to the mathematical model. In presented relationships, a subscript (l) marks the liquid phase and (s) denotes the solid phase.

The sum of the volume and mass fractions are

$$f_\mathrm{l} + f_\mathrm{s} = 1, \tag{20}$$

$$\xi_\mathrm{l} + \xi_\mathrm{s} = 1. \tag{21}$$

The density of a mixture consisting of two phases is meant as

$$\rho = \xi_\mathrm{l}\rho_\mathrm{l} + \xi_\mathrm{s}\rho_\mathrm{s}. \tag{22}$$

The relationships between the mass and volume fractions in liquid and solid phases are calculated with

$$f_\mathrm{l} = \frac{\rho_\mathrm{l}\xi_\mathrm{l}}{\rho} \tag{23}$$

and

$$f_\mathrm{s} = \frac{\rho_\mathrm{s}\xi_\mathrm{s}}{\rho}. \tag{24}$$

The velocity vector of mixture is estimated as a sum of velocities of the considered phases

$$\vec{W} = f_\mathrm{l}\vec{W}_\mathrm{l} + f_\mathrm{s}\vec{W}_\mathrm{s}. \tag{25}$$

Similarly to the definition of the velocity vector, the total enthalpy in the enthalpy equation is divided into the enthalpy of the liquid phase and the solid phase

$$\widehat{H} = f_\mathrm{l}\widehat{H}_\mathrm{l} + f_\mathrm{s}\widehat{H}_\mathrm{s}. \tag{26}$$

There are four possibilities to classify the velocity of the liquid and solid phase in a phase change region: (i) the solid phase possesses the same velocity as the liquid phase – e.g. substances like wax or glass, (ii) the velocities of two phases are different, (iii) the velocity of the solid phase is constant and (iv) the velocity of the solid phase equals zero. In order to avoid a very complex description of interactions between two moving phases, in the current work the last case is considered. Moreover, in the region between liquid and solid phase the dendritic model is supposed [18].

Since conservation equation of mass can be used in unchanged form, the momentum equation (2) and the

enthalpy equation (15) are enhanced by additional terms to enable the modelling of phase change phenomena.

3.1. Conservation equation of momentum with phase transition

The momentum equation that considers phase transition comes into existence after summation of the momentum equation for liquid and solid phase

$$\rho\left[\frac{\partial\vec{W}}{\partial t}+\left(\vec{W}\cdot\nabla\right)\vec{W}\right]=-\nabla p+\nabla\cdot\tau+\vec{F}-\vec{R}. \tag{27}$$

With the last term on the right side, changes in the fluid velocity within the phase transition region and the velocity of the solid phase are modelled

$$\vec{R}=\frac{\eta}{K}\left(\vec{W}-\vec{W}_{\mathrm{s}}\right). \tag{28}$$

In Eq. (28) K describes the Carman–Kozeny porosity model

$$K=K_0\frac{f_{\mathrm{l}}^3}{\left(1-f_{\mathrm{l}}\right)^2}. \tag{29}$$

The porosity model controls the deceleration of the liquid phase velocity within the phase transition region and ensures that the velocity of solid phase becomes zero. Ice crystals developing in a mushy region cause the deceleration of the fluid velocity. They affect some modifications of permeability in this region. Additionally, it is assumed that in the solid phase no internal tensions exist. The volume forces, which have their origin in velocity differences between both phases, can be neglected within the phase transition region due to very small values in comparison to the Darcy constant. Although, it is supposed that the structure of mushy region changes during high pressure treatment, the dependency of porosity on pressure and temperature is not taken into account.

3.2. Conservation equation of energy with phase transition

The conservation equation of energy

$$\begin{aligned}&\frac{\partial}{\partial t}\left(\rho\overline{H}\right)+\nabla\cdot\left(\rho\vec{W}\overline{H}\right)\\&\quad=\frac{\partial p}{\partial t}+\nabla\cdot\left(\lambda\nabla T\right)+\nabla\cdot\left(\left(\eta\left(\nabla\vec{W}+\left(\nabla\vec{W}\right)^{\mathrm{T}}\right.\right.\right.\\&\qquad\left.\left.\left.-\frac{2}{3}\nabla\cdot\vec{W}\delta\right)\right)\cdot\vec{W}\right)+\rho\vec{g}\cdot\vec{W}+S_k\end{aligned} \tag{30}$$

arises after addition of energy equations for several phases. The last term in Eq. (30)

$$S_k=-\frac{\partial}{\partial t}\left(\rho f_{\mathrm{l}}\widetilde{H}\right)-\nabla\cdot\left(\rho f_{\mathrm{l}}\vec{W}_{\mathrm{l}}\widetilde{H}\right) \tag{31}$$

describes the crystallization enthalpy released during freezing and thawing. In above presented source term the crystallization enthalpy is calculated with

$$\widetilde{H}=\int_{T_{\mathrm{s}}}^{T_{\mathrm{l}}}\left(c_{p_{\mathrm{l}}}-c_{p_{\mathrm{s}}}\right)\mathrm{d}T+L_{\mathrm{f}}. \tag{32}$$

Generally the crystallization enthalpy can be seen as a sum of the latent enthalpy L_{f} and the difference between the enthalpies of fluid and solid phases. The source term S_k can be written in the form of Eq. (31) after both terms of the total enthalpy on the left side of Eq. (15) are replaced by Eq. (26), whereby, the enthalpy of the liquid phase equals

$$\widehat{H}_{\mathrm{l}}=\int_{T_{\mathrm{s}}}^{\mathrm{T}}c_{pl}\,\mathrm{d}T+\frac{\vec{W}_{\mathrm{l}}^2}{2}+\widetilde{H}=h_{\mathrm{l}}+\frac{\vec{W}_{\mathrm{l}}^2}{2}+\widetilde{H} \tag{33}$$

and the enthalpy of the solid phase has following form:

$$\widehat{H}_{\mathrm{s}}=\int_{T_{\mathrm{s}}}^{\mathrm{T}}c_{ps}\,\mathrm{d}T+\frac{\vec{W}_{\mathrm{s}}^2}{2}=h_{\mathrm{s}}+\frac{\vec{W}_{\mathrm{s}}^2}{2}. \tag{34}$$

Consequently the left side of the enthalpy equation takes the form

$$\begin{aligned}\mathrm{LSG}=&\underline{\frac{\partial}{\partial t}\left(\rho f_{\mathrm{s}}h_{\mathrm{s}}+\rho f_{\mathrm{l}}h_{\mathrm{l}}\right)+\frac{\partial}{\partial t}\left(\rho f_{\mathrm{s}}\frac{\vec{W}_{\mathrm{s}}^2}{2}+\rho f_{\mathrm{l}}\frac{\vec{W}_{\mathrm{l}}^2}{2}\right)}\\&\underline{+\nabla\cdot\left(\rho f_{\mathrm{s}}\vec{W}_{\mathrm{s}}h_{\mathrm{s}}+\rho f_{\mathrm{l}}\vec{W}_{\mathrm{l}}h_{\mathrm{l}}\right)+\nabla\cdot\left(\rho f_{\mathrm{s}}\vec{W}_{\mathrm{s}}\frac{\vec{W}_{\mathrm{s}}^2}{2}+\rho f_{\mathrm{l}}\vec{W}_{\mathrm{l}}\frac{\vec{W}_{\mathrm{l}}^2}{2}\right)}\\&\underline{\underline{+\frac{\partial}{\partial t}\left(\rho f_{\mathrm{l}}\widetilde{H}\right)+\nabla\cdot\left(\rho f_{\mathrm{l}}\vec{W}_{\mathrm{l}}\widetilde{H}\right)}}.\end{aligned} \tag{35}$$

The addition of terms with the thermal and kinetic enthalpy leads to the expression on the left side of Eq. (30) and to the source term (31), respectively.

The equation system is completed with a function of phase transition

$$f_{\mathrm{l}}=\begin{cases}1, & \text{if } H>H_{\mathrm{l}},\\ \frac{H-H_{\mathrm{s}}}{H_{\mathrm{l}}-H_{\mathrm{s}}}, & \text{if } H_{\mathrm{s}}<H<H_{\mathrm{l}},\\ 0, & \text{if } H<H_{\mathrm{s}}\end{cases} \tag{36}$$

and the equation of state for pressurized medium

$$\rho=\rho(T,p). \tag{37}$$

The phase transition function takes values between 1 and 0. If the enthalpy of a substance exceeds the liquidus enthalpy then the value $f_{\mathrm{l}}=1$ indicates the liquid phase. In contrast, if the enthalpy is lower than the solidus enthalpy than $f_{\mathrm{l}}=0$.

4. Dimensional analysis of the high pressure process

The high pressure treatment of bio-substances is affected by the large number of internal and external parameters. The dimensional analysis gives the possibility to reduce their number and to generalize the statement about the process mechanisms and phenomena. The dimensionless numbers or groups that describe the high pressure process can be achieved using algebraic equations, differential equations or relevance lists [25]. In the current contribution the dimensionless description of the high pressure process

and the determination of dimensionless numbers is derived from the governing differential equations.

4.1. Dimensional analysis for liquid substances

The high pressure supported phase transition takes place due to specific temperature and pressure conditions in a closed and kept at a constant temperature or as adiabatically considered high pressure chamber. The classical high pressure processing consists of three phases – see Fig. 3. The compression is realised in the time t_1, the pressure holding phase in the time t_2 and a decompression in the time t_3. During these steps of high pressure process different thermo-fluid-dynamical phenomena occur. As presented in works of Pehl et al. [8,9] and Hartmann and Delgado [11], the fluid flow in the chamber is strongly affected by forced convection during compression. On the other hand free convection dominates pressure holding phase.

The pressure can be built up or reduced either by the supply/discharge of additional portion of pressure medium or by piston movement. Fig. 4 illustrates the possibilities of the high pressure generation in the chamber.

The dimensional analysis of governing equations is started for the case with forced convection and phase change. Since the pressure plays a key role in momentum and energy equation, one assumption is taken for its better handling. The total pressure is known as a sum of the static and dynamic pressure

$$p_{\text{tot}} = p_{\text{stat}} + p_{\text{dyn}} \tag{38}$$

with

$$p_{\text{dyn}} = \frac{1}{2}\rho W^2. \tag{39}$$

An exact analysis of the conservation equations shows that in the momentum equation the dynamic pressure and in the energy equation the static pressure is responsible for description of the fluid flow and the temperature increase caused by compression respectively. This assumption has a crucial consequence for dimensional analysis.

4.1.1. Dimensionless conservation equation of mass

The conservation equation of mass for two-dimensional problem becomes dimensionless with the following dimensionless values:

$$\rho^* = \frac{\rho}{\rho_0} = 0(1), \tag{40}$$

$$t^* = \frac{tW_0}{L_0} = 0(1), \tag{41}$$

$$x^* = \frac{x}{L_0} = 0(1), \tag{42}$$

$$y^* = \frac{y}{D} = 0(1), \tag{43}$$

$$W_x^* = \frac{W_x}{W_0} = 0(1), \tag{44}$$

$$W_y^* = \frac{W_y}{\frac{W_0 D}{L_0}} = \frac{W_y L_0}{W_0 D} = 0(1). \tag{45}$$

In order to ensure that the dimensionless velocity of fluid in y-direction remains in the order of magnitude between 0 and 1, the relationship between W_y and W_0 is extended

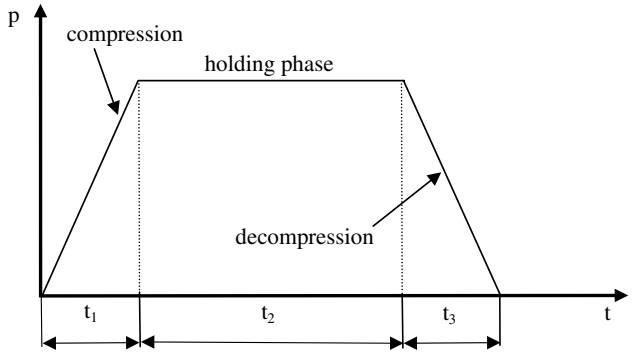

Fig. 3. The typical characteristics of the high pressure process.

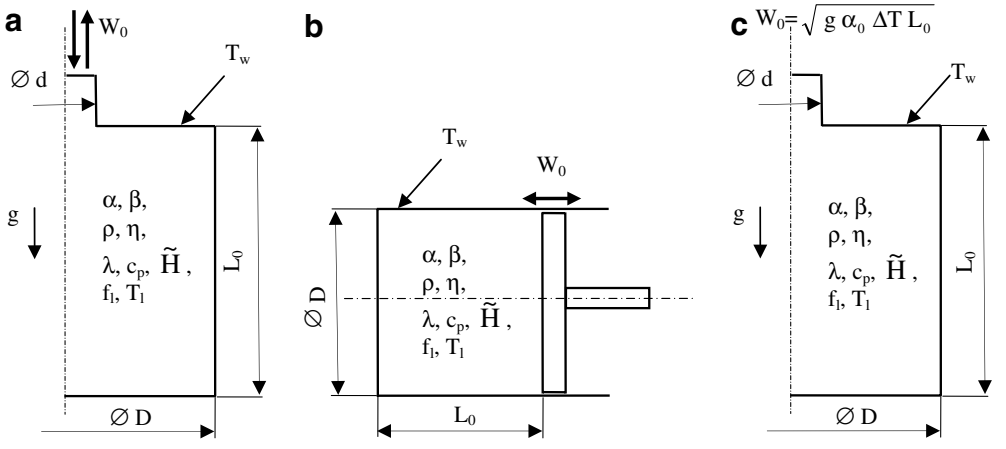

Fig. 4. High pressure chamber. (a) Compression due to additional mass transport into the pressure cell, (b) compression realised by piston movement, (c) system without the mass transport and piston movement – e.g. pressure changes due to phase transition.

with the geometrical ratio D/L. However this treatment of velocity components should be taken into account particularly in the case of the piston movement.

The implementation of the dimensionless variables in the conservation equation of mass and the division of both sides of equation with $(\rho_0 W_0/L_0)$ lead to following dimensionless form:

$$\frac{\partial \rho^*}{\partial t^*} + \frac{\partial}{\partial x^*}\left(\rho^* W_x^*\right) + \frac{\partial}{\partial y^*}\left(\rho^* W_y^*\right) = 0 \tag{46}$$

or

$$\frac{\partial \rho^*}{\partial t^*} + \nabla^* \cdot \left(\rho^* \vec{W}^*\right) = 0. \tag{47}$$

4.1.2. Dimensionless conservation equation of momentum

Using the dimensionless variables (40)–(45) in Eq. (27) and additionally considering further definitions

$$\eta^* = \frac{\eta}{\eta_0} = 0(1), \tag{48}$$

$$\eta'^* = \frac{\eta'}{\eta'_0} = 0(1), \tag{49}$$

$$K^* = \frac{K}{K_0} = 0(1), \tag{50}$$

$$\vec{g}^* = \frac{\vec{g}}{g_0} = 0(1), \tag{51}$$

and

$$p^* = \frac{p}{\rho_0 W_0^2} = 0(1) \tag{52}$$

results in the following conservation equation of momentum in the dimensionless form:

$$\begin{aligned}
&\rho^*\left[\frac{\partial W_x^*}{\partial t^*} + W_x^*\frac{\partial W_x^*}{\partial x^*} + W_y^*\frac{\partial W_x^*}{\partial y^*}\right] \\
&\quad = -\frac{\partial p^*}{\partial x^*} + 2\frac{\eta_0}{\rho_0 W_0 L_0}\frac{\partial}{\partial x^*}\left(\eta^*\frac{\partial W_x^*}{\partial x^*}\right) \\
&\qquad + \frac{\eta_0 L_0}{D^2 \rho_0 W_0}\frac{\partial}{\partial y^*}\left(\eta^*\frac{\partial W_x^*}{\partial y^*}\right) + \frac{\eta_0}{\rho_0 W_0 L_0}\frac{\partial}{\partial y^*}\left(\eta^*\frac{\partial W_y^*}{\partial x^*}\right) \\
&\qquad - \frac{2}{3}\frac{\eta_0}{\rho_0 W_0 L_0}\frac{\partial}{\partial x^*}\left(\eta^*\frac{\partial W_x^*}{\partial x^*}\right) - \frac{2}{3}\frac{\eta_0}{\rho_0 W_0 L_0}\frac{\partial}{\partial x^*}\left(\eta^*\frac{\partial W_y^*}{\partial y^*}\right) + \frac{L_0 g_0}{W_0^2}\rho^* g_x^* \\
&\qquad - \frac{\eta_0 L_0}{\rho_0 W_0 K_0}\frac{L_0}{L_0}\frac{\eta^*}{K^*}W_x^*, \\
&\rho^*\left[\frac{D}{L_0}\frac{\partial W_y^*}{\partial t^*} + \frac{D}{L_0}W_x^*\frac{\partial W_y^*}{\partial x^*} + \frac{D}{L_0}W_y^*\frac{\partial W_y^*}{\partial y^*}\right] \\
&\quad = -\frac{L_0}{D}\frac{\partial p^*}{\partial y^*} + \frac{\eta_0}{\rho_0 L_0 W_0}\frac{L_0}{D}\frac{\partial}{\partial x^*}\left(\eta^*\frac{\partial W_x^*}{\partial y^*}\right) + \frac{D}{L_0}\frac{\eta_0}{\rho_0 L_0 W_0}\frac{\partial}{\partial x^*}\left(\eta^*\frac{\partial W_y^*}{\partial x^*}\right) \\
&\qquad + 2\frac{\eta_0}{\rho_0 L_0 W_0}\frac{L_0}{D}\frac{\partial}{\partial y^*}\left(\eta^*\frac{\partial W_y^*}{\partial y^*}\right) - \frac{2}{3}\frac{\eta_0}{\rho_0 L_0 W_0}\frac{L_0}{D}\frac{\partial}{\partial y^*}\left(\eta^*\frac{\partial W_x^*}{\partial x^*}\right) \\
&\qquad - \frac{2}{3}\frac{\eta_0}{\rho_0 L_0 W_0}\frac{L_0}{D}\frac{\partial}{\partial y^*}\left(\eta^*\frac{\partial W_y^*}{\partial y^*}\right) - \frac{\eta_0 D L_0}{\rho_0 L_0 W_0 K_0}\frac{\eta^*}{K^*}W_y^*.
\end{aligned} \tag{53}$$

After some mathematical transformations and taking into consideration the definitions of well known dimensionless numbers like the Reynolds number

$$Re = \frac{W_0 L_0}{v_0} = \frac{\rho_0 W_0 L_0}{\eta_0} \tag{54}$$

that describes the relationship of convective and diffusive momentum transfer, the Froude number

$$Fr = \frac{W_0^2}{L_0 g}, \tag{55}$$

which designates the proportion of inertial force to gravitational force and the Darcy number

$$Da = \frac{K_0}{L_0^2}, \tag{56}$$

that characterizes the porosity of the medium at the solidification front, the final version of the momentum equation in 2D space can be written

$$\begin{aligned}
&\rho^*\left[\frac{\partial W_x^*}{\partial t^*} + W_x^*\frac{\partial W_x^*}{\partial x^*} + W_y^*\frac{\partial W_x^*}{\partial y^*}\right] \\
&\quad = -\frac{\partial p^*}{\partial x^*} + \frac{1}{Re}\left[2\frac{\partial}{\partial x^*}\left(\eta^*\frac{\partial W_x^*}{\partial x^*}\right) + \frac{L_0^2}{D^2}\frac{\partial}{\partial y^*}\left(\eta^*\frac{\partial W_x^*}{\partial y^*}\right)\right. \\
&\qquad \left. + \frac{\partial}{\partial y^*}\left(\eta^*\frac{\partial W_y^*}{\partial x^*}\right) - \frac{2}{3}\frac{\partial}{\partial x^*}\left(\eta^*\frac{\partial W_x^*}{\partial x^*}\right) - \frac{2}{3}\frac{\partial}{\partial x^*}\left(\eta^*\frac{\partial W_y^*}{\partial y^*}\right)\right] \\
&\qquad + \frac{1}{Fr}\rho^* g_x^* - \frac{1}{DaRe}\frac{\eta^*}{K^*}W_x^*, \\
&\rho^*\left[\frac{D}{L_0}\frac{\partial W_y^*}{\partial t^*} + \frac{D}{L_0}W_x^*\frac{\partial W_y^*}{\partial x^*} + \frac{D}{L_0}W_y^*\frac{\partial W_y^*}{\partial y^*}\right] \\
&\quad = -\frac{L_0}{D}\frac{\partial p^*}{\partial y^*} + \frac{1}{Re}\left[\frac{L_0}{D}\frac{\partial}{\partial x^*}\left(\eta^*\frac{\partial W_x^*}{\partial y^*}\right) + \frac{D}{L_0}\frac{\partial}{\partial x^*}\left(\eta^*\frac{\partial W_y^*}{\partial x^*}\right)\right. \\
&\qquad \left. + 2\frac{L_0}{D}\frac{\partial}{\partial y^*}\left(\eta^*\frac{\partial W_y^*}{\partial y^*}\right) - \frac{2}{3}\frac{L_0}{D}\frac{\partial}{\partial y^*}\left(\eta^*\frac{\partial W_x^*}{\partial x^*}\right) - \frac{2}{3}\frac{L_0}{D}\frac{\partial}{\partial y^*}\left(\eta^*\frac{\partial W_y^*}{\partial y^*}\right)\right] \\
&\qquad - \frac{1}{DaRe}\frac{D}{L_0}\frac{\eta^*}{K^*}W_y^*.
\end{aligned} \tag{57}$$

4.1.3. Dimensionless conservation equation of energy

The dimensionless conservation equation of energy is prepared with the dimensionless variables introduced for previous equations. Solely, an exception is taken for pressure. Like mentioned above, in the dimensionless energy equation only the hydrostatic pressure is considered (the effect of the dynamic pressure on the energy balance is assumed to be negligible). In order to achieve the value in the order of magnitude of 0(1), the pressure is normalized with initial amount of the density, the heat capacity and the temperature

$$p^* = \frac{p}{\rho_0 c_{p0} T_0} = 0(1). \tag{58}$$

Additionally, some new definitions of dimensionless variables are necessary

$$T^* = \frac{T}{T_0} = 0(1), \tag{59}$$

$$h^* = \frac{h}{c_{p0} T_0} = 0(1), \tag{60}$$

$$\lambda^* = \frac{\lambda}{\lambda_0} = 0(1), \tag{61}$$

$$f_1^* = f_1 = 0(1), \tag{62}$$

$$\widetilde{H}^* = \frac{\widetilde{H}}{L_f} = 0(1). \tag{63}$$

Considering the dimensionless numbers, the energy equation for 2D-cases is obtained

$$\begin{aligned}
&\rho^* \left[\frac{\partial h^*}{\partial t^*} + Ec \frac{\partial}{\partial t^*} \left(\frac{W_x^{*^2}}{2} \right) + Ec \frac{D^2}{L_0^2} \frac{\partial}{\partial t^*} \left(\frac{W_y^{*^2}}{2} \right) + W_x^* \frac{\partial h^*}{\partial x^*} \right. \\
&\quad + W_y^* \frac{\partial h^*}{\partial y^*} + Ec W_x^* \frac{\partial}{\partial x^*} \left(\frac{W_x^{*^2}}{2} \right) + Ec \frac{D^2}{L_0^2} W_x^* \frac{\partial}{\partial x^*} \left(\frac{W_y^{*^2}}{2} \right) \\
&\quad \left. + Ec W_y^* \frac{\partial}{\partial y^*} \left(\frac{W_x^{*^2}}{2} \right) + Ec \frac{D^2}{L_0^2} W_y^* \frac{\partial}{\partial y^*} \left(\frac{W_y^{*^2}}{2} \right) \right] \\
&\quad = \frac{\partial p^*}{\partial t^*} + \frac{1}{PrRe} \left[\frac{\partial}{\partial x^*} \left(\lambda^* \frac{\partial T^*}{\partial x^*} \right) + \frac{L_0^2}{D^2} \frac{\partial}{\partial y^*} \left(\lambda^* \frac{\partial T^*}{\partial y^*} \right) \right] \\
&\qquad + \frac{Ec}{Re} \left\{ W_x^* \frac{\partial}{\partial x^*} \eta^* \left[2 \frac{\partial W_x^*}{\partial x^*} - \frac{2}{3} \left(\frac{\partial W_x^*}{\partial x^*} + \frac{\partial W_y^*}{\partial y^*} \right) \right] \right. \\
&\qquad + W_y^* \frac{\partial}{\partial x^*} \eta^* \left[\frac{L_0}{D} \frac{\partial W_x^*}{\partial y^*} + \frac{D}{L_0} \frac{\partial W_y^*}{\partial x^*} \right] \\
&\qquad + W_x^* \frac{\partial}{\partial y^*} \eta^* \left[\frac{L_0^2}{D^2} \frac{\partial W_x^*}{\partial y^*} + \frac{\partial W_y^*}{\partial x^*} \right] \\
&\qquad \left. + W_y^* \frac{\partial}{\partial y^*} \eta^* \left[2 \frac{\partial W_y^*}{\partial y^*} - \frac{2}{3} \left(\frac{\partial W_x^*}{\partial x^*} + \frac{\partial W_y^*}{\partial y^*} \right) \right] \right\} \\
&\qquad + \frac{Ec}{Fr} \rho^* g_x^* \cdot W_x^* - \frac{1}{Ste} \frac{\partial}{\partial t^*} \left(\rho^* f_1^* \widetilde{H}^* \right) \\
&\qquad - \frac{1}{Ste} W_{xl}^* \frac{\partial}{\partial x^*} \left(\rho^* f_1^* \widetilde{H}^* \right) - \frac{1}{Ste} W_{yl}^* \frac{\partial}{\partial y^*} \left(\rho^* f_1^* \widetilde{H}^* \right).
\end{aligned} \tag{64}$$

The dimensionless numbers are defined as the Eckert number

$$Ec = \frac{W_0^2}{c_{p0} T_0}, \tag{65}$$

which describes relationship of kinetic energy and enthalpy and supplies a measure for the compressibility of the pressurized fluid, the Prandtl number

$$Pr = \frac{\eta_0 c_{p0}}{\lambda_0}, \tag{66}$$

that expresses the ratio between momentum and thermal diffusivity and the Stefan number

$$Ste = \frac{c_{p0} \Delta T}{L_f}, \tag{67}$$

which characterizes the phase transition. The product of dimensionless numbers Re and Pr gives the Peclet number

$$Pe = RePr. \tag{68}$$

4.2. Dimensionless conservation equations – pure free convection

During the pressure holding step the fluid flow in the high pressure chamber is formed by free convection. The free convection is developed due to density changes of pressurized medium. These changes are generated particularly through temperature gradients. The dimensionless description of processes with free convection and that with forced convection differs in some points. Because of the absence of the inlet velocity of the fluid into the container a special view on the definition of a new characteristic velocity by free convection is required. Thus, the new characteristic reference velocity is calculated with

$$W_0 = \sqrt{g \alpha_0 \Delta T L_0}. \tag{69}$$

Moreover, much longer process time in comparison to compression phase induces a special treatment of the dimensionless time. Eq. (41) proceeds from the maximum compression time t_c as a characteristic time

$$t^* = \frac{t}{t_c} = 0(1). \tag{70}$$

Simultaneously multiplication and division of this equation with a new process time for the holding phase t_p results in

$$t^* = \frac{t}{t_p} \frac{t_p}{t_c} = \frac{t}{t_p} t_s^* = 0(1). \tag{71}$$

Thus, with the dimensionless time $t_s^* = t_p / t_c$ a time conversion for long lasting processes takes place, e.g., the pressure holding phase during sterilization of bio-substance or freezing/thawing at constant pressure.

4.2.1. Dimensionless conservation equation of mass – pure free convection

The dimensionless conservation equation of mass for compressible media with free convection is identical to Eq. (47).

4.2.2. Dimensionless conservation equation of momentum – pure free convection

In systems with free convection the fluid flow is driven by the volume force $\nabla \rho \cdot \vec{g}$. For compressible media where the density is taken as a function of pressure and temperature $\rho = \rho(p, T)$ the modified Boussinesq approximation serves for appropriate description of the density difference

$$(\rho - \rho_0) = \rho_0 (\beta \Delta p - \alpha \Delta T) = \rho_0 (\beta (p - p_0) - \alpha (T - T_0)). \tag{72}$$

This approach requires consideration of dimensionless values of the thermal expansion coefficient

$$\alpha^* = \frac{\alpha}{\alpha_0} = 0(1) \tag{73}$$

and the compressibility coefficient

$$\beta^* = \frac{\beta}{\beta_0} = 0(1). \tag{74}$$

Thus, the dimensionless momentum equation in x-direction (gravity) is written as follow:

$$\begin{aligned}
&\rho^*\left[\frac{\partial W_x^*}{\partial t^*} + W_x^*\frac{\partial W_x^*}{\partial x^*} + W_y^*\frac{\partial W_x^*}{\partial y^*}\right] \\
&\quad = -\frac{\partial p^*}{\partial x^*} + \frac{1}{Re}\left[2\frac{\partial}{\partial x^*}\left(\eta^*\frac{\partial W_x^*}{\partial x^*}\right) + \frac{L_0^2}{D^2}\frac{\partial}{\partial y^*}\left(\eta^*\frac{\partial W_x^*}{\partial y^*}\right)\right. \\
&\qquad \left. + \frac{\partial}{\partial y^*}\left(\eta^*\frac{\partial W_y^*}{\partial x^*}\right) - \frac{2}{3}\frac{\partial}{\partial x^*}\left(\eta^*\frac{\partial W_x^*}{\partial x^*}\right) - \frac{2}{3}\frac{\partial}{\partial x^*}\left(\eta^*\frac{\partial W_y^*}{\partial y^*}\right)\right] \\
&\qquad + \frac{g_x^*}{Re^2}\Pi_A - \frac{1}{DaRe}\frac{\eta^*}{K^*}W_x^*.
\end{aligned} \tag{75}$$

Comparing with Eq. (57), other dimensionless numbers appear in the momentum equation. The Galileo number

$$Ga = \frac{g_0 L_0^3}{\nu^2} = \frac{Re^2}{Fr} \tag{76}$$

describes the relationship between the gravitational and viscous force, the characteristic number

$$\Pi_A = \frac{(\alpha_0\Delta T + \beta_0\Delta p)g_0 L_0^3}{\nu_0^2} = Ga(\alpha_0\Delta T + \beta_0\Delta p), \tag{77}$$

characterizes the buoyancy effect. In the pressure holding phase (constant pressure conditions) the dimensionless number Π_A changes into the Grashof number

$$Gr = \frac{\alpha\Delta T g_0 L_0^3}{\nu^2} = Ga\alpha\Delta T. \tag{78}$$

Furthermore, in the momentum equation in x-direction the term (Gr/Re^2) occurs. Such a ratio of the Gr and Re number is known as the Archimedes number

$$Ar = \frac{Gr}{Re^2}. \tag{79}$$

It balances the gravitational force to viscous force. Analysing the Ar number can be stated that in the systems in which the fluid flow is characterized with $Re \gg 1$ the effect of buoyancy force is significantly reduced.

4.2.3. Dimensionless conservation equation of energy – pure free convection

The derivation of the dimensionless conservation equation of energy for the systems with free convection leads to

$$\begin{aligned}
&\rho^*\left[\frac{\partial h^*}{\partial t^*} + Ec\frac{\partial}{\partial t^*}\left(\frac{W_x^{*2}}{2}\right) + Ec\frac{D^2}{L_0^2}\frac{\partial}{\partial t^*}\left(\frac{W_y^{*2}}{2}\right) + W_x^*\frac{\partial h^*}{\partial x^*}\right. \\
&\quad + W_y^*\frac{\partial h^*}{\partial y^*} + EcW_x^*\frac{\partial}{\partial x^*}\left(\frac{W_x^{*2}}{2}\right) + Ec\frac{D^2}{L_0^2}W_x^*\frac{\partial}{\partial x^*}\left(\frac{W_y^{*2}}{2}\right) \\
&\quad \left. + EcW_y^*\frac{\partial}{\partial y^*}\left(\frac{W_x^{*2}}{2}\right) + Ec\frac{D^2}{L_0^2}W_y^*\frac{\partial}{\partial y^*}\left(\frac{W_y^{*2}}{2}\right)\right] \\
&\quad = \frac{\partial p^*}{\partial t^*} + \frac{1}{GrPr}\left[\frac{\partial}{\partial x^*}\left(\lambda^*\frac{\partial T^*}{\partial x^*}\right) + \frac{L_0^2}{D^2}\frac{\partial}{\partial y^*}\left(\lambda^*\frac{\partial T^*}{\partial y^*}\right)\right] \\
&\qquad + \frac{Ec}{Re}\left\{W_x^*\frac{\partial}{\partial x^*}\eta^*\left[2\frac{\partial W_x^*}{\partial x^*} - \frac{2}{3}\left(\frac{\partial W_x^*}{\partial x^*} + \frac{\partial W_y^*}{\partial y^*}\right)\right]\right. \\
&\qquad + W_y^*\frac{\partial}{\partial x^*}\eta^*\left[\frac{L_0}{D}\frac{\partial W_x^*}{\partial y^*} + \frac{D}{L_0}\frac{\partial W_y^*}{\partial x^*}\right] W_x^*\frac{\partial}{\partial y^*}\eta^*\left[\frac{L_0^2}{D^2}\frac{\partial W_x^*}{\partial y^*} + \frac{\partial W_y^*}{\partial x^*}\right] \\
&\qquad \left. + W_y^*\frac{\partial}{\partial y^*}\eta^*\left[2\frac{\partial W_y^*}{\partial y^*} - \frac{2}{3}\left(\frac{\partial W_x^*}{\partial x^*} + \frac{\partial W_y^*}{\partial y^*}\right)\right]\right\} \\
&\qquad + \frac{Ec}{Fr}\rho^* g_x^*\cdot W_x^* - \frac{1}{Ste}\frac{\partial}{\partial t^*}\left(\rho^* f_1^*\widetilde{H}^*\right) \\
&\qquad - \frac{1}{Ste}W_{xl}^*\frac{\partial}{\partial x^*}\left(\rho^* f_1^*\widetilde{H}^*\right) - \frac{1}{Ste}W_{yl}^*\frac{\partial}{\partial y^*}\left(\rho^* f_1^*\widetilde{H}^*\right).
\end{aligned} \tag{80}$$

The dimensionless group $GrPr$ is defined as the Rayleigh number

$$Ra = GrPr. \tag{81}$$

This number described the ratio of the diffusive to the convective heat transfer.

4.3. Dimensional analysis of enthalpy equation for solid substance

Considering the phase changes in solid bio-substances at constant pressure and assuming that there are no dislocations inside the material, the system of equations is reduced significantly. Thus, the enthalpy equation in the 2D case can be written as

$$\frac{\partial \rho h}{\partial t} = \frac{\partial}{\partial x}\left(\lambda\frac{\partial T}{\partial x}\right) + \frac{\partial}{\partial y}\left(\lambda\frac{\partial T}{\partial y}\right) - \frac{\partial}{\partial t}\left(\rho f_l\widetilde{H}\right). \tag{82}$$

Using already defined dimensionless variables the dimensionless form of the enthalpy equation for solid substances is achieved

$$\begin{aligned}
\frac{\partial \rho^* h^*}{\partial t^*} &= Fo\left[\frac{\partial}{\partial x^*}\left(\lambda^*\frac{\partial T^*}{\partial x^*}\right) + \frac{L_0^2}{D^2}\frac{\partial}{\partial y^*}\left(\lambda^*\frac{\partial T^*}{\partial y^*}\right)\right] \\
&\quad - \frac{\Theta}{Ste}\frac{\partial}{\partial t^*}\left(\rho^* f_1^*\widetilde{H}^*\right).
\end{aligned} \tag{83}$$

In this equation the dimensionless temperature ratio Θ is calculated as

$$\Theta = \frac{\Delta T}{T_0} = \frac{T_0 - T_l}{T_0} = 1 - \frac{T_l}{T_0} \tag{84}$$

and the Fourier number is defined with

$$Fo = \frac{\lambda_0}{\rho_0 c_{p0} L_0^2}t_p. \tag{85}$$

4.4. Dimensional analysis of the thermal energy equation

For direct analysis of an influence of several thermo-fluid-dynamical mechanisms on temperature growth during the high pressure treatment (e.g. compression), the dimensional analysis of the thermal energy equation is carried out. The thermal energy equation is written as follows:

$$c_{\mathrm{p}}\rho\frac{\mathrm{D}T}{\mathrm{D}t}=\alpha T\frac{\mathrm{D}p}{\mathrm{D}t}+\nabla\cdot(\lambda\nabla T)+\eta\Phi-\rho\widetilde{H}\frac{Df_{\mathrm{l}}}{\mathrm{D}t}. \tag{86}$$

After transformation into the dimensionless form we achieve

$$\begin{aligned}
&c_{\mathrm{p}}^{*}\rho^{*}\left[\frac{\partial T^{*}}{\partial t^{*}}+W_{x}^{*}\frac{\partial T^{*}}{\partial x^{*}}+W_{y}^{*}\frac{\partial T^{*}}{\partial y^{*}}\right]\\
&\quad=\Pi_{T}\left\{\alpha^{*}T^{*}\frac{\partial p^{*}}{\partial t^{*}}+\alpha^{*}T^{*}\left[W_{x}^{*}\frac{\partial p^{*}}{\partial x^{*}}+W_{y}^{*}\frac{\partial p^{*}}{\partial y^{*}}\right]\right\}\\
&\qquad+\frac{1}{RePr}\left[\frac{\partial}{\partial x^{*}}\left(\lambda^{*}\frac{\partial T^{*}}{\partial x^{*}}\right)+\frac{L_{0}^{2}}{D^{2}}\frac{\partial}{\partial y^{*}}\left(\lambda^{*}\frac{\partial T^{*}}{\partial y^{*}}\right)\right]\\
&\qquad+\frac{Ec}{Re}\left\{2\eta^{*}\left[\left(\frac{\partial W_{x}^{*}}{\partial x^{*}}\right)^{2}+\left(\frac{\partial W_{y}^{*}}{\partial y^{*}}\right)^{2}+\frac{1}{2}\left(\frac{L_{0}^{2}}{D^{2}}\frac{\partial W_{x}^{*}}{\partial y^{*}}+\frac{\partial W_{y}^{*}}{\partial x^{*}}\right)^{2}\right]\right.\\
&\qquad\left.-\frac{2}{3}\eta^{*}\left[\frac{\partial W_{x}^{*}}{\partial x^{*}}+\frac{\partial W_{y}^{*}}{\partial y^{*}}\right]\right\}-\frac{\Theta}{Ste}\frac{\partial}{\partial t^{*}}\left(\rho^{*}f_{\mathrm{l}}^{*}\widetilde{H}^{*}\right)\\
&\qquad-\frac{Ec\Theta}{Ste}\left[W_{xl}^{*}\frac{\partial}{\partial x^{*}}\left(\rho^{*}f_{\mathrm{l}}^{*}\widetilde{H}^{*}\right)-W_{yl}^{*}\frac{\partial}{\partial y^{*}}\left(\rho^{*}f_{\mathrm{l}}^{*}\widetilde{H}^{*}\right)\right]
\end{aligned} \tag{87}$$

The thermal energy equation shows clearly that in systems with low velocities of fluid, where $Ec\to 0$, the dissipation function possesses a negligible influence on the temperature increase during compression stage. Moreover, it can be seen that the dimensionless number

$$\Pi_{T}=\alpha_{0}T_{0} \tag{88}$$

is responsible for the description of the temperature changes in pressurized medium. This number can be also derived from the formula for the computation of temperature increase due to compression in adiabatic systems

$$\left(\frac{\mathrm{d}T}{\mathrm{d}p}\right)\Big|_{\mathrm{s}}=\frac{\alpha Tv}{c_{\mathrm{p}}}=\frac{\alpha T}{\rho c_{\mathrm{p}}}. \tag{89}$$

Further, the temperature increase in adiabatic systems can be expressed in dimensionless form as

$$\left(\frac{\mathrm{d}T^{*}}{\mathrm{d}p^{*}}\right)\Big|_{\mathrm{s}}=\underbrace{\alpha_{0}T_{0}}_{\Pi_{T}}\frac{\alpha^{*}T^{*}}{\rho^{*}c_{\mathrm{p}}^{*}}. \tag{90}$$

5. Discussion of the dimensional analysis

The analysis of the dimensionless governing equations allows to state, which phenomena have a significant influence and which plays a minor role on the thermo-fluid-dynamics of high pressure processes. A large value of the dimensionless group, points out an elevated importance of these mechanisms on the momentum and heat transfer in high pressure autoclaves. In contrast, if dimensionless parameters become very small values, it means that these terms can be neglected.

First, the dimensionless groups that contain the Ec number are analysed. Because of very low velocities of fluid in the majority of cases such dimensionless groups (e.g. Eq. (91)) can be neglected.

$$\Pi_{\mathrm{D}}=\frac{Ec}{Re}=\frac{\frac{W_{0}^{2}}{c_{p0}T_{0}}}{\frac{\rho_{0}L_{0}W_{0}}{\eta_{0}}}=\frac{W_{0}v_{0}}{c_{p0}T_{0}}. \tag{91}$$

Since the Re number depends on the characteristic velocity proportionally, it can not sufficiently balance the decrease (low velocities) expressed by the Ec number. It can be seen that if $Re\to 0$, the Ec number converges to 0 quadratically. Thus, the effect of dissipation is neglected in such cases. Contrarily, at high velocities of fluid different effects commence. In the situation when $Re\to\infty$ the Ec number reaches also very high values and the dissipation function gains in importance.

Because of compression, the temperature increase of a pressurized medium is observed. The dimensionless description of this phenomenon

$$\Pi_{T}\alpha^{*}T^{*}=\alpha_{0}T_{0}\alpha^{*}T^{*} \tag{92}$$

is present in the equation of thermal energy (Eq. (87)). It shows that greater values of the thermal expansion coefficient cause higher temperature of medium due to compression. For instance, the temperature increase of water, ethanol and acetic acid can be compared. At the same initial temperature, ethanol and acetic acid warm up much more than water. This phenomenon is caused by their larger thermal expansion coefficients. Additionally, the higher initial temperature of the process, the higher increase of the temperature of a pressurized medium is obtained.

In the cases with phase transitions, the crystallization enthalpy is a significant component of the conservation equation of energy. The dimensionless group

$$\frac{1}{Ste}=\frac{L_{\mathrm{f}}}{c_{p0}\Delta T} \tag{93}$$

quantifies an influence of the latent heat on the energy balance. The higher latent heat of a substance, the higher contribution of this term to the energy balance is noted. Consequently, one of many technological advantages of phase transitions in food under high pressure bases on the fact, that with increasing pressure the crystallization enthalpy decreases. For instance, in comparison to the latent heat at normal pressure the latent heat of water at 200 MPa is approximately 30% lower.

The contribution of the volume forces in the energy equation is expressed by

$$\Pi_{\mathrm{V}}=\frac{Ec}{Fr}=\frac{\frac{W_{0}^{2}}{c_{p0}T_{0}}}{\frac{W_{0}^{2}}{g_{0}L_{0}}}=\frac{g_{0}L_{0}}{c_{p0}T_{0}}. \tag{94}$$

For the high pressure treatment of bio-substances the product $c_{p0}T_{0}$ is higher than $g_{0}L_{0}$. Thus, the dimensionless

Table 1
Estimated values of dimensionless numbers/groups

Dimensionless number/group	Order of magnitude
Ec	10^{-8}
$1/Pe$	10^{-3}
$1/Ra$	10^{-7}
$\Pi_D = Ec/Re$	10^{-10}
$\Pi_V = Ec/Fr$	10^{-6}
$\Pi_P = 1/DaRe$	1
$1/Re$	10^{-2}
$1/Fr$	10^{3}
$g^*\Pi_A/Re^2$	10^{3}
Fo	10^{-2}
$1/Ste$	1
Θ/Ste	10^{-1}
Π_T	10^{-2}

number Π_V becomes very small and the influence of this volume force on the energy balance can be neglected.

The relationship of the diffusive to convective heat transport for the cases with forced convection is written as

$$\frac{1}{PrRe} = \frac{1}{Pe} = \frac{\lambda_0}{c_{p0}\eta_0}\,\frac{\eta_0}{\rho_0 W_0 L_0} = \frac{a_0}{W_0 L_0} \tag{95}$$

and with free convection is described through

$$\frac{1}{PrGr} = \frac{1}{Ra} = \frac{\lambda_0}{c_{p0}\eta_0}\,\frac{\eta_0^2}{\rho_0^2\alpha_0 g_0 \Delta T L_0^3} = \frac{a_0 v_0}{\alpha_0 g_0 \Delta T L_0^3}. \tag{96}$$

The dimensionless group in the last term of the conservation equation of momentum

$$\Pi_P = \frac{1}{DaRe} = \frac{L_0^2}{K_0}\,\frac{\eta_0}{\rho_0 W_0 L_0} = \frac{L_0 v_0}{K_0 W_0} \tag{97}$$

characterizes the resistance force that decelerates the velocity of a substance during freezing. As soon as the liquid medium changes into the solid state, the permeability of the mushy region decreases proportionally to the amount of the solid volume fraction. In pure solid phase the permeability K_0 reaches its smallest value and the velocity of completely frozen part is zero. The theoretical analysis of this dimensionless group shows that by very high velocities of fluid the resistance force can be insufficient to decelerate or completely stop the fluid flow. In such a case this term would lose its importance in the momentum equation. Unlike, the deceleration of the fluid is more effective if Re converges to zero.

Table 1 presents the estimated orders of magnitude for several dimensionless numbers and groups in the governing equations. These values are calculated with the thermophysical properties of water and the characteristic lengths of laboratory high pressure chambers (see [24]).

6. Conclusions

The high pressure technology opens new possibilities for processing and product development of bio-substances. In order to understand the mechanisms and phenomena occurring during high pressure treatment, the fundamental analysis of dimensionless governing equations describing the processes with forced and free convection is carried out. The influence of geometrical ratio of the chamber (L/D) is also taken into account for dimensional analysis of velocity components in x-, and y-direction. Because of technological advantages of phase change under high pressure conditions, the mathematical description of the phase transitions in momentum and energy equation is considered. The high pressure treatment of bio-substances consists of three steps. During compression and decompression process the forced convection dominates the fluid flow in the vessel. The free convection is the major mechanism during the pressure holding phase. From the differential equations, the dimensionless numbers: Pr, Re, Ec, Fr, Ste and Da, which describe forced convection with phase change at high pressure are acquired. In the dimensionless description of the processes with dominating free convection, the Gr number describes additionally the influence of the buoyancy force. The temperature increase caused by compression is expressed with the dimensionless number Π_V. This number depends on the thermal expansion coefficient and the initial temperature of a pressurized medium. In systems with low velocities of a pressurized fluid, the irreversible transformation of the kinetic energy into the thermal energy (the dissipation function) can be neglected. The phase change in solid substances can be described with Θ, Fo and Ste number.

The dimensional analysis presented in the current paper gives a general overview of thermo-fluid-dynamical mechanisms of high pressure processes. The determination of dimensionless numbers is of great importance for transformation of laboratory investigations and results into the industrial scale.

References

[1] P.W. Bridgman, The coagulation of albumen by pressure, J. Biol. Chem. 19 (1914) 511–512.
[2] P.W. Bridgman, The thermal conductivity of liquids under pressure, Proc. Am. Acad. Arts Sci. 59 (1923) 141–169.
[3] M.F. San Martin, G.V. Barbosa-Canovas, B.G. Swanson, Food processing by high hydrostatic pressure, Crit. Rev. Food Sci. Nutr. 42 (6) (2002) 627–645.
[4] J.C. Cheftel, Effects of high hydrostatic pressure on food constituents: an overview, in: C. Balny, R. Hayashi, K. Heremans, P. Masson (Eds.), High Pressure and Biotechnology, Colloque. INSERM/John Libbey and Co. Ltd, London, 1992, pp. 195–209.
[5] D. Knorr, Advantages, opportunities and challenges of high hydrostatic pressure application to food systems, in: R. Hayashi, C. Balny (Eds.), Proceedings of the International Conference on High Pressure Bioscience and Biotechnology, High Pressure Bioscience and Biotechnology Kyoto, Japan, 1996, pp. 279–287.
[6] P. Först, F. Werner, A. Delgado, The viscosity of water – especially at subzero degrees centigrade, Rheologica Acta 39 (2000) 566–573.
[7] P. Först, F. Werner, A. Delgado, On the pressure dependence of the viscosity of aqueous sugar solutions, Rheol. Acta 41 (2002) 369–374.
[8] M. Pehl, A. Delgado, An in situ technique to visualize temperature and velocity fields in liquid biotechnical substances at high pressure, in: H. Ludwig (Ed.), Advances in High Pressure Bioscience and Biotechnology, Springer, Heidelberg, 1999, pp. 519–522.

[9] M. Pehl, F. Werner, A. Delgado, First visualization of temperature fields in liquids at high pressure, Exp. Fluids 29 (2000) 302–304.
[10] A. Delgado, Chr. Hartmann, Pressure treatment of food: instantaneous but not homogeneous effect, in: R. Winter (Ed.), Proceedings of the 2nd International Conference on High Pressure Bioscience and Biotechnolgy, Advances in High Pressure Bioscience and Biotechnolgy Dortmund, 2003, pp. 459–464.
[11] C. Hartmann, A. Delgado, Numerical simulation of convective and diffusive transport effects on a high-pressure-induced inactivation process, Biotechnol. Bioengi. 79 (1) (2002) 94–104.
[12] C. Hartmann, A. Delgado, J. Szymczyk, Convective and diffusive transport effects in a high pressure induced inactivation process of packed food, J. Food Eng. 59 (2003) 33–44.
[13] P.W. Bridgman, Water in the liquid and five solid forms under pressure, Proc. Am. Acad. Arts Sci. 47 (1912) 439–558.
[14] J.C. Cheftel, J. Levy, E. Dumay, Pressure-assisted freezing and thawing: principles and potential applications, Food Rev. Int. 16 (4) (2000) 453–483.
[15] M.T. Kalichevsky, D. Knorr, P.J. Lillford, Potential food applications of high-pressure effects on ice-water transitions, Trends Food Sci. Technol. 6 (1995) 253–259.
[16] V.R. Voller, An overview of numerical methods for solving phase change problems, in: W.J. Minkowycz, E.M. Sparrow (Eds.), Advances in Numerical Heat Transfer, Taylor & Francis, Washington, DC, 1997, pp. 341–380 (Chapter 9).
[17] V.R. Voller, M. Cross, N.C. Markatos, An enthalpy method for convection/diffusion phase change, Int. J. Numer. Methods Eng. 24 (1987) 271–284.
[18] V.R. Voller, A.D. Brent, C. Prakasch, The modelling of heat mass and solute transport in solidification systems, Int. J. Heat Mass Transfer 32 (9) (1989) 1719–1731.
[19] C.R. Swaminathan, V.R. Voller, Towards a general numerical scheme for solidification systems, Int. J. Heat Mass Transfer 40 (12) (1997) 2859–2868.
[20] W.D. Bennon, F.P. Incropera, A continuum model for momentum, heat and species transport in binary solid–liquid phase change systems – I. Model formulation, Int. J. Heat Mass Transfer 30 (10) (1987) 2161–2170.
[21] W.D. Bennon, F.P. Incropera, A continuum model for momentum, heat and species transport in binary solid–liquid phase change systems – II. Application to solidification in a rectangular cavity, Int. J. Heat Mass Transfer 30 (10) (1987) 2171–2187.
[22] J. Ni, F.P. Incropera, Extension of the continuum model for transport phenomena occurring during metal alloy solidification – I. The conservation equations, Int. J. Heat Mass Transfer 38 (7) (1995) 1271–1284.
[23] J. Ni, F.P. Incropera, Extension of the continuum model for transport phenomena occurring during metal alloy solidification – II. Microscopic considerations, Int. J. Heat Mass Transfer 38 (7) (1995) 1285–1296.
[24] W. Kowalczyk, Chr. Hartmann, A. Delgado, Modelling and numerical simulation of convection driven high pressure induced phase changes, Int. J. Heat Mass Transfer 47 (5) (2004) 1079–1089.
[25] J. Stichlmair, Kennzahlen und Ähnlichkeitsgesetze im Ingenieurwesen, Vertrieb: Altos-Verlag Doris Stichlmair, Essen, 1990.